# Analysis of the Relationship Between Operational Mastery Process and Balance Capability in Daily Life for Unstable Personal Vehicles

Kenta Nomura, Kazuki Obata(✉), and Masami Iwase

Tokyo Denki University, 5-Senju Adachi, Tokyo 120-8551, Japan
obata@ctrl.fr.dendai.ac.jp

**Abstract.** This research aims to analyze a relation between balance ability in daily life and process of attaining a maneuvering skill for unstable vehicles such as unicycle, Segway and balance board. For the analysis, the subjects have carried out the balance ability test on the flat ground and the holding balance experiment on the balance board. As a result, the balance ability on a balance board correlated with the static balance ability. Hence, a model, which integrated human with balance board, has been derived in order to analyze relation between balance ability of both legs and control performance. In conclusion, the model which integrated human with balance board, have been stabilized by control system design.

**Keywords:** Human balance ability · Unstable vehicle · Proficiency support

## 1 Introduction

Since Segway [1] was developed in 2001; the personal mobility vehicle of handstand pendulum type (PMV) has been paid its attention to as a new means of transportation. PMV is smaller and more mobile than bicycles and bikes, so it can be used indoors as well as middle-range movement. In addition, the decrease in $CO_2$ emission is reported when the use of PMV is replaced by a part of the short-range movement of the car [2]. In this way, PMV is highly convenient and an energy-saving vehicle. However, PMV is stabilized by control because structure is instability such as two wheels and one wheel. Also, since the occupant largely moves the center of gravity when operating the PMV, and the occupant own self also needs to maintain an unstable posture [3]. Therefore, in addition to stabilization of PMV by control, balance ability of occupant is required, when riding in PMV.


V.H. Duy et al. (eds.), *AETA 2017 - Recent Advances in Electrical Engineering and Related Sciences: Theory and Application*, Lecture Notes in Electrical Engineering 465,
https://doi.org/10.1007/978-3-319-69814-4_38

Many studies in human balance ability have been done. The balance ability is roughly divided into two: "static balance ability" which maintains the center of gravity within the base of support, "dynamic balance ability" where the base of support also moves according to the movement of the center of gravity [4]. The static balance ability is necessary for maintenance of static posture such as in standing positions, and the dynamic balance ability is need when keep stable posture with center of gravity movement such as the time of a walk or sport [5]. These ability is essential in everyday life. The balance ability tends to decline due to the reduction of muscular strength, vestibular system, vision and so on, due to age and activity level decline [6]. It is thought that opportunities to use PMV as a means of transporting such users whose balance ability has declined will increase [7]. However, balance ability in everyday life and the relations of the operation mastery of unstable PMV are not elucidated.

Therefore, the balance ability in the everyday life and the relations of the operation proficiency for an unstable vehicle are analyzed using the unstable vehicle that balance ability is required. The clarification of two relations allow the improvement of the balance ability by the operation mastery.

This research is aimed for the analysis of the operation skill process of an unstable vehicle and the relations of the human balance ability. This research intends for a balance board to use in sports training. Since the balance board balances in the standing position, it is able to be expected to have a relationship with the balance ability in daily life. In this paper, an integrated model of humans and balance boards are derived, and the control performance is related the balance holding ability of the left and right legs. The results of the model are compared and considered from the results of the correlation analysis of the balance holding test on the floor surface and the balance holding test on the balance board.

## 2 Model Derivation

The fact, that the static balance ability is closely related to the balance ability of the balance board, is suggested by the correlation analysis between the balance ability test on the balance board and the balance ability test in everyday life [8]. Therefore, the reasons for the correlation between the static balance ability and the balance ability on the balance board need to be analyzed. It is considered that the relationship between the static balance ability and the balance ability on the balance board by analyzing the human balance action on the balance board. Performing a balance operation is well studied in the field of control as a problem of stabilization. A typical example is an inverted pendulum. In other words, from the viewpoint of control, it is possible to treat the balance operation of a person on the balance board as a stabilization problem of how to stabilize the human controller. Therefore, the balance board and human integrated model are stabilized by deriving the model of the balance board and the human and designing the control system of the human model. It is considered the relationship between the static balance ability and the balance ability on the balance board

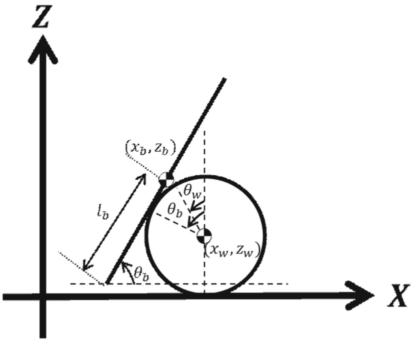


**Fig. 1.** Integration model of balance board

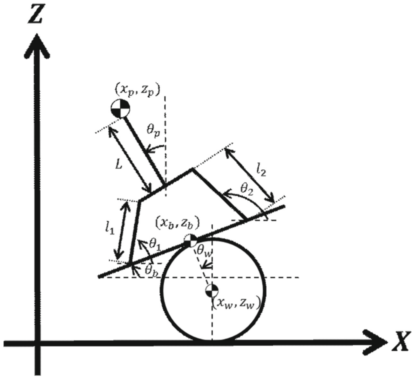


**Fig. 2.** Integration model of balance board and human

by relating the balance holding ability of the left and right feet to the control performance.

In this section, a model is derived that integrates the model of the balance board and the human model using Projection Method [9]. The model of the balance board is shown in Fig. 1, and the integration model of balance board and human is shown in Fig. 2.

## 2.1 Balance Board Model

The cylinder and the plate are restrained and the equation of motion of the balance board are derived. The physical parameters of the balance board are shown in Table 1, and the variables are shown in Table 2.

**Table 1.** The physical parameters of the balance board

| Symbols | Descriptions [Unit] |
|---|---|
| $m_w$ | Mass of cylinder [kg] |
| $m_b$ | Mass of plate [kg] |
| $J_w$ | Moment of inertia of cylinder $[\mathrm{kg} \cdot \mathrm{m}^2]$ |
| $J_b$ | Moment of inertia of plate $[\mathrm{kg} \cdot \mathrm{m}^2]$ |
| $r$ | Radius of cylinder [m] |
| $l_b$ | Distance from the center of gravity of the plate to the edge [m] |
| $c$ | Viscosity coefficient $[\mathrm{Nm} \cdot \mathrm{s/rad}]$ |
| $g$ | Gravitational acceleration $[\mathrm{m/s^2}]$ |

From Fig. 1, since the subsystem is a cylinder and a plate, the equations of motion in a free state are derived without on each constraints. Defining the

**Table 2.** The variables of the balance board

| Symbols | Descriptions [Unit] |
|---|---|
| $\theta_w$ | Rotation angle of cylinder [rad] |
| $\theta_b$ | Rotation angle of plate [rad] |
| $(x_w, z_w)$ | Center of gravity of cylinder [m] |
| $(x_b, z_b)$ | Center of gravity of plate [m] |

generalization speed as $\boldsymbol{v}_b$, generalized mass as $\boldsymbol{M}_b$, generalization power as $\boldsymbol{h}_b$, the equation of motion in the free state is expressed as (1).

$$\begin{aligned} \boldsymbol{M_b}\dot{\boldsymbol{v}}_b &= \boldsymbol{h}_b \\ \boldsymbol{M}_b &:= \mathrm{diag}(\mathrm{J_w}, \mathrm{J_b}, \mathrm{m_w}, \mathrm{m_w}, \mathrm{m_b}, \mathrm{m_b}) \\ \boldsymbol{v}_b &:= \left[\dot{\theta}_w,\, \dot{\theta}_b,\, \dot{x}_w,\, \dot{z}_w,\, \dot{x}_b,\, \dot{z}_b\right]^T \\ \boldsymbol{h}_b &:= \left[-c_b\dot{\theta}_w,\, -c_b\dot{\theta}_b,\, 0,\, -m_w g,\, 0,\, -m_b g\right]^T \end{aligned} \tag{1}$$

Define the constraint condition as "the cylinder does not idle", "the cylinder does not float", "the plate and the cylinder do not slip", and the constraint condition is time-differentiated for speed constraint. The detailed content of restraint is omitted due to space limitations. In addition, a new velocity vector $\dot{\boldsymbol{q}}_b$ (hereinafter: contact speed) after constraint is expressed by (2).

$$\dot{\boldsymbol{q}}_b := \left[\dot{\theta}_w,\, \dot{\theta}_b\right]^T \tag{2}$$

The orthogonal complement matrix $\boldsymbol{D}_b$ is derived by partially differentiating the velocity constraint with the contact velocity $\dot{\boldsymbol{q}}_b$.

$$\boldsymbol{D}_b = \begin{bmatrix} 1 & 0 \\ 0 & 1 \\ -r & 0 \\ 0 & 0 \\ -r\cos\theta_b - r & -r(\theta_b - \theta_w)\sin\theta_b \\ -r\sin\theta_b & r(\theta_b - \theta_w)\cos\theta_b \end{bmatrix} \tag{3}$$

Therefore, the equation of movement of the balance board is represented only by the degrees of freedom after being constrained as (4).

$$\boldsymbol{D}_b^T \boldsymbol{M}_b \boldsymbol{D}_b \ddot{\boldsymbol{q}}_b + \boldsymbol{D}_b^T \boldsymbol{M}_b \dot{\boldsymbol{D}}_b \dot{\boldsymbol{q}}_b = \boldsymbol{D}_b^T \boldsymbol{h}_b \tag{4}$$

### 2.2 Integrates the Model of the Balance Board and the Human

The equation of movement of the integrated model is derived by constraining the balance board model and the human model. The physical parameters of the human are shown in Table 3, and the variables are shown in Table 4.

**Table 3.** The physical parameters of the human

| Symbols | Descriptions [Unit] |
|---|---|
| $m_p$ | Mass of head [kg] |
| $J_p$ | Moment of inertia of the head [$\mathrm{kg \cdot m^2}$] |
| $s_1$ | Waist width [m] |
| $s_2$ | Width of both feet [m] |
| $L$ | Distance from waist to head [m] |
| $c$ | Viscosity coefficient [$\mathrm{Nm \cdot s/rad}$] |
| $g$ | Gravitational acceleration [$\mathrm{m/s^2}$] |

**Table 4.** The variables of the human

| Symbols | Descriptions [Unit] |
|---|---|
| $l_1$ | Length of left foot [m] |
| $l_2$ | Length of right foot [m] |
| $\theta_1$ | Rotation angle of left foot [rad] |
| $\theta_2$ | Rotation angle of right foot [rad] |
| $\theta_p$ | Head rotation angle [rad] |
| $(x_p, z_p)$ | Head center of gravity position [m] |

From Fig. 2, the subsystem is a balance board and a human. Therefore, a free state equation of movement about the integrated model is and newly derived by summarizing the equations of movement of the balance board in Sect. 2.1 and the movement equations of the state of humans. Defining the generalization speed as $\boldsymbol{v}_p$, generalized mass as $\boldsymbol{M}_p$, generalization power as $\boldsymbol{h}_p$, the equation of movement in the free state is expressed as (5).

$$\boldsymbol{M_p}\dot{\boldsymbol{v}}_p = \boldsymbol{h}_p \tag{5}$$

$$\boldsymbol{M}_p := \mathrm{diag}(\mathrm{J_p}, \mathrm{m_p}, \mathrm{m_p})$$

$$\boldsymbol{v}_p := \left[\dot{\theta}_p,\ \dot{x}_p,\ \dot{z}_p\right]^T \tag{6}$$

$$\boldsymbol{h}_p := \left[-c_p\dot{\theta}_p,\ 0,\ -m_p g\right]^T \tag{7}$$

Next, (8) is derived by transforming (4) for the balance board model.

$$\begin{aligned}
\boldsymbol{D}_b^T \boldsymbol{M}_b \boldsymbol{D}_b \ddot{\boldsymbol{q}}_b &= \boldsymbol{D}_b^T \boldsymbol{h}_b - \boldsymbol{D}_b^T \boldsymbol{M}_b \dot{\boldsymbol{D}}_b \dot{\boldsymbol{q}}_b \\
\boldsymbol{M}_B \dot{\boldsymbol{v}}_B &= \boldsymbol{h}_B \\
\boldsymbol{M}_B :&= \boldsymbol{D}_b^T \boldsymbol{M}_b \boldsymbol{D}_b \\
&= \begin{bmatrix} M_{B11} & M_{B12} \\ M_{B21} & M_{B22} \end{bmatrix} \\
\boldsymbol{h}_B :&= \boldsymbol{D}_b^T (\boldsymbol{h}_B - \boldsymbol{M}_b \dot{\boldsymbol{D}}_b \dot{\boldsymbol{q}}_b) \\
&= \left[h_{B1}\ h_{B2}\right]^T
\end{aligned} \tag{8}$$

The integrations of (5) and (8) lead (9).

$$\boldsymbol{M}\dot{\boldsymbol{v}} = \boldsymbol{h} \tag{9}$$

$$\boldsymbol{M} := \begin{bmatrix} M_{B11} & M_{B12} & 0 & 0 & 0 \\ M_{B21} & M_{B22} & 0 & 0 & 0 \\ 0 & 0 & J_p & 0 & 0 \\ 0 & 0 & 0 & m_p & 0 \\ 0 & 0 & 0 & 0 & m_p \end{bmatrix} \tag{10}$$

$$\dot{\boldsymbol{v}} := \left[\ddot{\theta}_w, \ddot{\theta}_b, \ddot{\theta}_p, \ddot{x}_p, \ddot{z}_p\right]^T \tag{11}$$

$$\boldsymbol{h} := \left[h_{B1}, h_{B2}, -c_p\dot{\theta}_p, 0, -m_p g\right]^T \tag{12}$$

The constraint condition is defined as "Human foot is in contact with the balance board". A detailed content of restraint is omitted due to the space limitations. Also define a new contact velocity $\dot{\boldsymbol{q}}$ after constraint.

$$\dot{\boldsymbol{q}} := \left[\dot{\theta}_w, \dot{\theta}_b, \dot{l}_1, \dot{l}_2, \dot{\theta}_1\right]^T \tag{13}$$

A partial differentiation of speed constraint with the contact speed $\dot{\boldsymbol{q}}$ leads to orthogonal complement matrix $\boldsymbol{D}$. From the set forth above, the equation of movement of the integrated model is as follows

$$\boldsymbol{D}^T\boldsymbol{M}\boldsymbol{D}\ddot{\boldsymbol{q}} + \boldsymbol{D}^T\boldsymbol{M}\dot{\boldsymbol{D}}\dot{\boldsymbol{q}} = \boldsymbol{D}^T\boldsymbol{h}. \tag{14}$$

## 3 Control System Design

Using the derived integrated model as a control object, a control system is designed that stabilizes humans on the balance board.

### 3.1 Linearization

Linearize the nonlinear equation of movement of the derived integrated model using Taylor expansion. The derived nonlinear equation of movement is expressed as follows

$$\dot{\boldsymbol{x}} = f(\boldsymbol{x}, \boldsymbol{u}). \tag{15}$$

By setting the equilibrium point to $\boldsymbol{x}_0$ and the input at the equilibrium point to $\boldsymbol{u}_0$, the following equation holds.

$$0 = f(\boldsymbol{x}_0, \boldsymbol{u}_0) \tag{16}$$

The equilibrium points are shown as follows

$$\boldsymbol{q}_0 = \left[{}^0\theta_w, {}^0\theta_b, {}^0l_1, {}^0l_2, {}^0\theta_1\right]^T$$
$$\dot{\boldsymbol{q}}_0 = \left[{}^0\dot{\theta}_w, {}^0\dot{\theta}_b, {}^0\dot{l}_1, {}^0\dot{l}_2, {}^0\dot{\theta}_1\right]^T$$
$$\ddot{\boldsymbol{q}}_0 = \left[{}^0\ddot{\theta}_w, {}^0\ddot{\theta}_b, {}^0\ddot{l}_1, {}^0\ddot{l}_2, {}^0\ddot{\theta}_1\right]^T$$

When the equilibrium point is the stable $\dot{\boldsymbol{q}}_0$ is shown as follows.

$$\begin{aligned}\dot{\boldsymbol{q}}_0 &= \left[{}^0\dot{\theta}_w,\, {}^0\dot{\theta}_b,\, {}^0\dot{l}_1,\, {}^0\dot{l}_2,\, {}^0\dot{\theta}_1\right]^T \\ &= \left[0.0,\, 0.0,\, 0.0,\, 0.0,\, 0.0\right]^T\end{aligned}$$

The combination of equilibrium point $\boldsymbol{q}_0$ and the equilibrium point input $\boldsymbol{u}_0$ are infinite numbers. This means that the balance holding posture is different depending on the person.

Taylor expansion of the left side of (14) leads to the following expression.

$$\boldsymbol{f}(\boldsymbol{q}, \dot{\boldsymbol{q}}, \ddot{\boldsymbol{q}}) = \boldsymbol{f}(\boldsymbol{q}_0, \dot{\boldsymbol{q}}_0, \ddot{\boldsymbol{q}}_0) + \frac{\partial \boldsymbol{f}}{\partial \boldsymbol{q}}(\boldsymbol{q} - \boldsymbol{q}_0) + \frac{\partial \boldsymbol{f}}{\partial \dot{\boldsymbol{q}}}(\dot{\boldsymbol{q}} - \dot{\boldsymbol{q}}_0) + \frac{\partial \boldsymbol{f}}{\partial \ddot{\boldsymbol{q}}}(\ddot{\boldsymbol{q}} - \ddot{\boldsymbol{q}}_0) \quad (17)$$

In the similar way, when Taylor expansion is applied to the right side, the following equation is derived.

$$\boldsymbol{f}(\boldsymbol{u}) = \boldsymbol{f}(\boldsymbol{u}_0) + \frac{\partial \boldsymbol{f}}{\partial \boldsymbol{u}}(\boldsymbol{u} - \boldsymbol{u}_0) \quad (18)$$

From (17) and (18), near the equilibrium point is regarded as the following linear equations. However, it is defined as $\boldsymbol{M}_l := \frac{\partial \boldsymbol{f}}{\partial \ddot{\boldsymbol{q}}}$, $\boldsymbol{N}_l := \frac{\partial \boldsymbol{f}}{\partial \dot{\boldsymbol{q}}}$, $\boldsymbol{G}_l := \frac{\partial \boldsymbol{f}}{\partial \boldsymbol{q}}$, $\boldsymbol{H}_l := \frac{\partial \boldsymbol{f}}{\partial \boldsymbol{u}}$, $\ddot{\bar{\boldsymbol{q}}} := (\ddot{\boldsymbol{q}} - \ddot{\boldsymbol{q}}_0)$, $\dot{\bar{\boldsymbol{q}}} := (\dot{\boldsymbol{q}} - \dot{\boldsymbol{q}}_0)$, $\bar{\boldsymbol{q}} := (\boldsymbol{q} - \boldsymbol{q}_0)$ and $\bar{\boldsymbol{u}} := (\boldsymbol{u} - \boldsymbol{u}_0)$.

$$\boldsymbol{M}_l\ddot{\bar{\boldsymbol{q}}} + \boldsymbol{N}_l\dot{\bar{\boldsymbol{q}}} + \boldsymbol{G}_l\bar{\boldsymbol{q}} = \boldsymbol{H}_l\bar{\boldsymbol{u}} \quad (19)$$

In addition, the following expressions are led by changing into the equation of state in (19).

$$\begin{aligned}\dot{\boldsymbol{x}} &= \boldsymbol{A}\boldsymbol{x} + \boldsymbol{B}\boldsymbol{u} \\ \frac{d}{dt}\begin{bmatrix}\bar{\boldsymbol{q}} \\ \dot{\bar{\boldsymbol{q}}}\end{bmatrix} &= \begin{bmatrix}\boldsymbol{Z}(5,5) & \boldsymbol{I}(5,5) \\ -\boldsymbol{M}_l^{-1}\boldsymbol{G}_l & -\boldsymbol{M}_l^{-1}\boldsymbol{N}_l\end{bmatrix}\begin{bmatrix}\bar{\boldsymbol{q}} \\ \dot{\bar{\boldsymbol{q}}}\end{bmatrix} + \begin{bmatrix}\boldsymbol{Z}(5,3) \\ \boldsymbol{M}_l^{-1}\boldsymbol{H}_l\end{bmatrix}\end{aligned}$$

### 3.2 Model-Based Stabilizing Control Based on State Dependent Riccati Equation

The feedback matrix $\boldsymbol{F}$ is derived from the system matrix $\boldsymbol{A}, \boldsymbol{B}$ and the weight matrix $\boldsymbol{Q}, \boldsymbol{R}$, and the integrated model is stabilized by state feedback. In the model shown in Fig. 2, since servos are not applied to $l_1, l_2, \theta_1$, so human form can not be preserved. Therefore, by adding inputs of $u_1, u_2, u_3$ to $l_1, l_2, \theta_1$, we try to stabilize while keeping the human model.

The equilibrium points of the integrated model were set as follows.

$$\begin{aligned}\boldsymbol{q}_0 &= \left[0.0,\, 0.0,\, 2.0,\, 2.0,\, \tfrac{\pi}{3}\right]^T \\ \dot{\boldsymbol{q}}_0 &= \left[0.0,\, 0.0,\, 0.0,\, 0.0,\, 0.0\right]^T \\ \ddot{\boldsymbol{q}}_0 &= \left[0.0,\, 0.0,\, {}^0u_1,\, {}^0u_2,\, {}^0u_3\right]^T\end{aligned}$$

By shifting the initial state $\boldsymbol{x}$ from the equilibrium point as shown below, the unified model was set up in an unstable situation.

$$\begin{aligned}\boldsymbol{x} &= \left[\theta_w,\, \theta_b,\, l_1,\, l_2,\, \theta_1,\, \dot{\theta}_w,\, \dot{\theta}_b,\, \dot{l}_1,\, \dot{l}_2,\, \dot{\theta}_1\right]^T \\ &= \left[0.0,\, \tfrac{\pi}{18},\, 2.0,\, 2.0,\, \tfrac{\pi}{3},\, 0.0,\, 0.0,\, 0.0,\, 0.0,\, 0.0\right]^T\end{aligned}$$

Weight matrix $\boldsymbol{Q}$, $\boldsymbol{R}$ for the determining feedback gain $\boldsymbol{F}$ were set as follows. This value was chosen by trial and error.

$$\begin{aligned}\boldsymbol{F} &= -\boldsymbol{R}^{-1}\boldsymbol{B}^T\boldsymbol{P} \\ \boldsymbol{Q} &= \mathrm{diag}(1000, 1000, 1, 1, 1, 1, 1, 1, 1, 1) \\ \boldsymbol{R} &= \mathrm{diag}(1, 1, 1)\end{aligned} \tag{20}$$

However, P is a real positive definite symmetric solution that satisfies the following formula.

$$\boldsymbol{PA} + \boldsymbol{A}^T\boldsymbol{P} - \boldsymbol{PBR}^{-1}\boldsymbol{BP} + \boldsymbol{Q} = 0$$

### 3.3 Verification of Simulation Result

The integrated model was numerically simulated for 8.0 s with step size of 0.01 s using 4th order Runge-Kutta method. The physical parameters used in the simulation are indicated in Table 5. The position of the cylinder is shown in Fig. 3.

**Table 5.** The physical parameters of the balance board

| Symbols | Descriptions [Unit] | Values |
|---|---|---|
| $m_w$ | Mass of cylinder [kg] | 0.5 |
| $m_b$ | Mass of plate [kg] | 1.0 |
| $m_p$ | Mass of head [kg] | 1.5 |
| $r$ | Radius of cylinder [m] | 1.0 |
| $L$ | Distance from waist to head [m] | 1.5 |
| $l_b$ | Distance from the center of gravity of the plate to the edge [m] | 3.0 |
| $J_w$ | Moment of inertia of cylinder [$\mathrm{kg \cdot m^2}$] | 0.25 |
| $J_b$ | Moment of inertia of board [$\mathrm{kg \cdot m^2}$] | 0.083 |
| $J_p$ | Moment of inertia of the head [$\mathrm{kg \cdot m^2}$] | 0.28 |
| $s_1$ | Length of waist [m] | 2.0 |
| $s_2$ | Width of both feet [m] | 4.0 |
| $c_b$ | Rolling friction coefficient [$\mathrm{Nm \cdot s/rad}$] | 0.001 |
| $c_p$ | Viscosity coefficient of joint [$\mathrm{Nm \cdot s/rad}$] | 0.002 |
| $g$ | Gravitational acceleration [$\mathrm{m/s^2}$] | 9.81 |

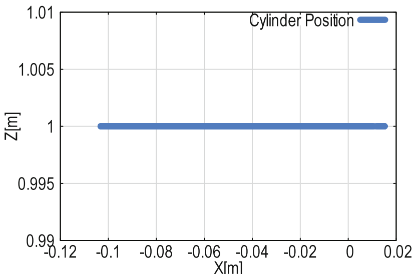


**Fig. 3.** The position of the cylinder

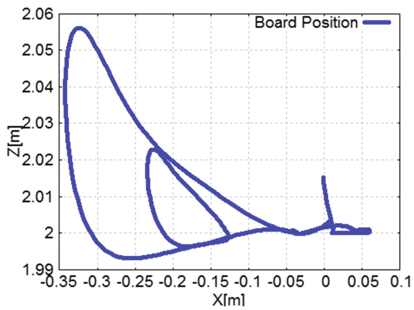


**Fig. 4.** The position of the board

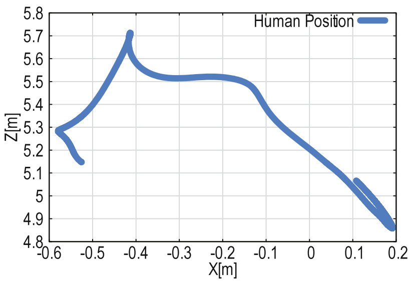


**Fig. 5.** The human position

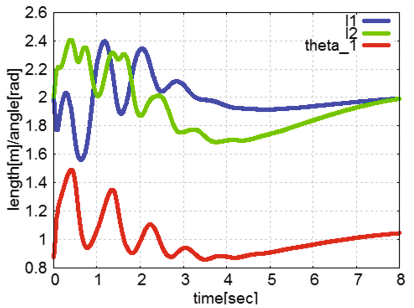


**Fig. 6.** The length and interior angle of a human foot

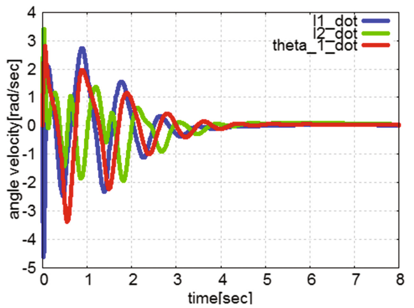


**Fig. 7.** The speed and angular velocity of a human foot

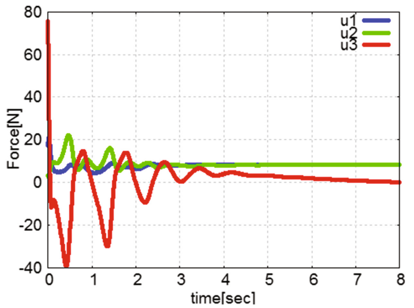


**Fig. 8.** The control input

The position of the board is shown in Fig. 4. The human position is shown in Fig. 5. The length and interior angle of a human foot are shown in Fig. 6. The speed and angular velocity of a human foot are shown in Fig. 7. The control input is shown in Fig. 8. The angle of a cylinder, a board and a human are shown in Fig. 9. The cylinder and plate angular velocity are shown in Fig. 10.

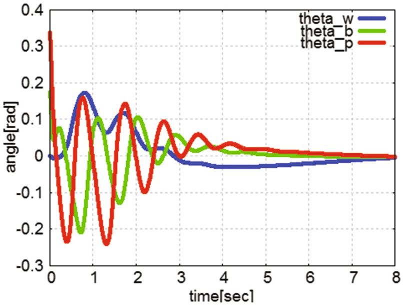


**Fig. 9.** The angle of a cylinder, a board, and a human

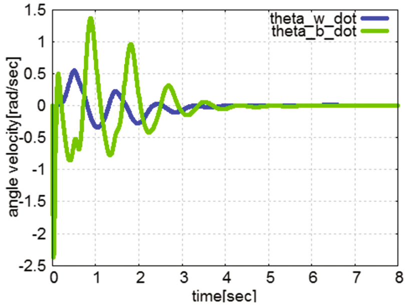


**Fig. 10.** Cylinder and plate angular velocity

Figures 6 and 9 indicate that the integrated model has converged to the equilibrium point $\boldsymbol{q}_0$. Also, Figs. 7 and 10 indicate that the speed converges to zero. From the set forth above, it was confirmed that the integrated model was stabilized.

## 4 Conclusion

In this research, the purpose of the analysis is to analyze the influence of balance ability in daily life on learning process for unstable vehicles such as unicycle, Segway, balance board and so on. For analysis, a control system for deriving an integrated model of human and balance board, and the stabilizing integrated model was designed. As future works, an extended models of left and right feet will be derived so as to relate the balance holding ability of left and right feet to the control performance. The relationship between the balance action of a person on the balance board and the static balance ability will be considered using the integrated model and the extended model of human and balance board.

## References

1. Segway Japan. http://www.segway-japan.net/
2. Suda, Y., Nakano, K., Tanaka, S., Hirasawa, T., Makino, H., Nakagawa, C., Hirayama, Y.: Prototype development of personal mobility vehicle and feasibility study for ecological and aging society. Prod. Res. **63**(2), 287–292 (2011)
3. Nakagawa, C., Morita, Y., Shintani, A., Ito, T.: Standing posture analysis of a human on a four-wheel stand-up-type personal mobility vehicle. Trans. JSME **82**(838), 16-00052 (2016)
4. Takagi, D., Nisida, Y.: Calf circumference and static balance using stationary posturography. J. Rehabil. Sci. Ser. Christopher Univ. **8**, 45–51 (2013)
5. Kubota, T., Kasuga, K., Fukutomi, K.: Effects of various habitual exercise routines on dynamic balance ability. Nat. Sci. **36**, 139–144 (2012). Graduate School of Education, Gifu University
6. Fujimoto Medical System: Advanced medical course, 30 June 2014. www.fujimoto.or.jp/tip-medicine/lecture-153/index.php. Accessed 7 July 2014

7. Tokyo Fire Department: Accident of the elderly seen from emergency transport data, 4 July 2014. www.tfd.metro.tokyo.jp/lfe/topics/201209/koureijiko.html. Accessed 7 July 2014
8. Nomura, K., Watanabe, T., Iwase, M.: Relation analysis between balance ability in daily life and process of attaining riding skill for unstable vehicles. In: Technical Papers of Annual Meeting, The 57th Japan Joint Automatic Control Conference. (2014)
9. Blajer, W.: A projection method approach to constrained dynamic analysis. J. Appl. Mech. **59**, 643–649 (1992)